JOURNAL OF MATERIALS SCIENCE 22 (1987) 419–428

The adhesive behaviour of poly(*p*-phenylene benzobisthiazole) (PBT)/epoxy composites

MENAS S. VRATSANOS, EDWIN L. THOMAS, RICHARD J. FARRIS
Department of Polymer Science and Engineering, University of Massachusetts, Amherst, Massachusetts 01003, USA

A modified scarf joint specimen was developed for characterizing the adhesive behaviour of poly(*p*-phenylene benzobisthiazole) (PBT) film/epoxy composites. This method subjected samples to varying amounts of normal stress (tensile or compressive) and shear stress. This resulted in the determination of two adhesive strengths; one in the absence of shear stress and one in the absence of normal stress. As a result, the dependence of the adhesive strength on the degree of normal stress was determined. The adhesive behaviour of PBT/epoxy composites was investigated at cure temperatures of 55, 85, 115 and 215°C. Adhesive strengths of 3.5 and 8.2 MPa were measured in the absence of shear and normal stress, respectively, for samples cured at 55° C. A decrease in adhesive strength with increasing cure temperature was attributed to residual cure and thermal stresses. The fracture of these composites was predominantly adhesive, resulting in a clean delamination of the PBT film from the epoxy surface. A modified Tsai–Wu failure criterion is suggested for these composites.

1. Introduction

High-performance composites are readily replacing traditional materials in structural applications. This is largely due to the fact that these composites offer outstanding mechanical properties when compared to metals on an equivalent weight basis. There are, however, some composite properties which are not always "high performance". One such deficiency is in the area of adhesion. Clearly, the success of a composite structure depends upon the degree of adhesion between the reinforcement and the matrix. Because structural components are rarely subjected to simple stress fields, it is important to understand the adhesive response of a composite to multi-axial loading geometries.

Previous research on carbon, graphite, and Kevlar 49 fibres has investigated the surface properties, adhesion characteristics and effect of surface treatment on adhesion for these fibres and their composites [1–4]. The mechanical characterization of these composites has involved various pull-out, lap shear and short beam shear experiments. While all three test methods assume a pure shear loading to determine adhesive strength, there are normal and residual thermal stresses present which can complicate the interpretation of the resulting mechanical data. In addition, simple beam theory can be inadequate for calculating the adhesive properties of composite structures. Some of these inadequacies have been pointed out by Sandorff [5]. In most cases corrections accounting for these non-idealities have not been performed.

Recently, Arcan *et al.* [6] developed a test method for applying uniform states of plane stress. This method allowed for varying the amount of normal and shear stress that samples experienced. While this method eliminated many experimental problems it could not be used in this study because of special material handling requirements. For this reason a modified scarf joint specimen was designed.

This paper will address the adhesive behaviour of poly(*p*-phenylene benzobisthiazole) (PBT) film/epoxy composites. PBT is a new high performance reinforcement not yet commercially available. Extensive mechanical and morphological studies of PBT have been performed [7–13]. The study of the adhesive behaviour of PBT fibres, however, has been limited to short beam shear experiments on PBT/epoxy unidirectional laminates and filament-wound composites. Typical adhesive strengths of 30 to 40 MPa have been reported [12, 13].

As a motivation for studying the adhesion of PBT films, it is suggested that from an engineering perspective it might be advantageous to design composite structures using a film or ribbon-based reinforcement rather than a fibre-based reinforcement. This would allow for higher volume fractions of reinforcement, easier lay-ups and might exploit the transverse properties of the film. This paper presents some preliminary results on the adhesive characterization of PBT film composites subjected to combined normal (tensile or compressive) and shear stresses using a modified scarf joint specimen.

2. Materials

PBT is an aromatic heterocyclic rigid-rod polymer developed under the Ordered Polymers Research Program at the US Air Force Wright-Patterson Materials Laboratory. PBT possesses many of the mechanical and thermal properties typical of polymers in the high performance class. Its chemical structure is given in Fig. 1.

0022–2461/87 $03.00 + .12

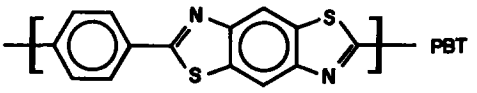

Figure 1 Chemical structure of poly(*p*-phenylene benzobisthiazole) (PBT).

Highly anisotropic uniaxial ribbons of PBT were dry-jet wet extruded from lyotropic liquid crystalline solutions of PBT in polyphosphoric acid by the Celanese Research Company. As evidence of its anisotropy, a secondary electron image (SEI) of a peeled PBT ribbon is shown in Fig. 2. The films were ~ 0.5 cm wide and $\sim 5\,\mu$m thick. Details regarding the extrusion conditions have been published elsewhere [10]. Typical mechanical properties of the as-extruded PBT film are given in Table I. The values reported in Table I have been corrected for the effect of machine compliance.

Epon 828, a DGEBA (diglycidyl ether of bisphenol-A) epoxy resin and 62 parts per hundred resin (p.h.r.) of V-40, an amino-polyamide curing agent, were chosen as the matrix system. Both materials were provided by the Shell Chemical Company. According to the equivalent weights reported in the Shell technical literature, this corresponds to an amine/epoxy stoichiometric ratio of 0.8. The chemical structure of Epon 828 is given in Fig. 3. The choice of V-40 as curing agent is based upon its use in adhesive applications [15–17]. V-40 is the product of the condensation of unsaturated fatty acids with triethylene tetramine. The mechanical properties of the neat V-40/Epon 828 epoxy system during cure have been published by Vratsanos and Farris [18, 19].

3. Experimental details

The extreme mechanical anisotropy along the extrusion direction made cutting and handling of the films a very delicate task. It was necessary to find an experimental apparatus which minimized the pressure applied to a composite laminate and minimized handling. For this reason the design of Arcan *et al.* [6] was not chosen.

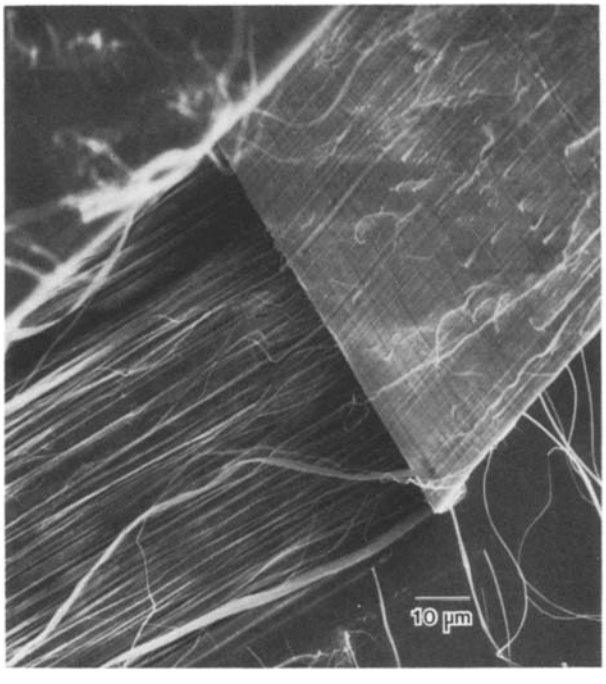

Figure 2 Secondary electron image (SEI) of a PBT ribbon peeled in the extrusion direction showing its anisotropic and fibrillar character.

TABLE I Mechanical properties of the as-extruded PBT film

Tensile modulus	130 GPa
Tensile strength	1 GPa*
Elongation to break	2%
Compressive strength	230 MPa†

* 1 cm gauge length.
† Determined by cantilever beam bending technique [14]

The modified scarf joint design allowed one to vary the relative amount of normal stress (tensile or compressive) to shear stress that the samples experienced. This experimental design satisfied the requirement of minimal handling of the PBT films and did not subject the PBT/epoxy composites to any significant pressure.

The advantage of the modified scarf joint geometry for an adhesive characterization is two-fold. First is the determination of two adhesive strengths; one in the absence of shear stress and one in the absence of normal stress. Second, the sensitivity of the adhesive strength to the degree of normal stress can be established. As noted, the lap shear and short beam shear tests ideally offer an interlaminar shear strength only.

Figs 4a and b illustrate the neat epoxy and PBT/epoxy composite samples, respectively. The following method was used to prepare the PBT/epoxy samples:

1. $\frac{3}{16}$ in. × $\frac{3}{16}$ in. cold rolled steel stock was machined into pieces measuring $\frac{13}{16}$ in. in length.
2. A $\frac{1}{8}$ in. hole was drilled into each steel piece at a precise distance, x, measured from the centre of the steel piece. The distance x ranged from $\frac{1}{32}$ to $\frac{5}{16}$ in.
3. The steel substrates were degreased by washing them in hexane, *p*-xylene and acetone.
4. Two steel substrates (each having a hole drilled at the same value of x) were then coated with a thin (10 to 30 μm) layer of the V-40/828 mixture.
5. A 1 in. ribbon of PBT was placed on one of the amine/epoxy coated steel substrates. The second coated steel piece was then placed on top of the PBT ribbon such that the $\frac{1}{8}$ in. holes were on opposite sides of the sample.
6. A very slight pressure was applied to the symmetrical composite sandwich.
7. The samples were cured at 55, 85, 115 or 215° C for 2.5 h. This was followed by a slow cool to room temperature.
8. Samples were then subjected to varying degrees of normal and shear stresses by virtue of the sample geometry.

In all cases testing was done at room temperature. In a similar fashion, samples without PBT were also prepared.

Tensile normal/shear stress testing was accomplished by pinning the steel substrates of the sample in specially designed sample holders. These sample holders were mounted in an Instron testing machine

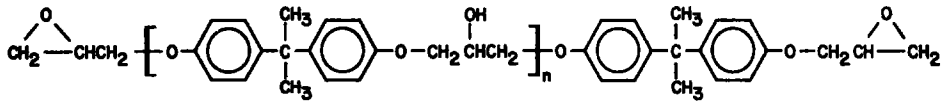

EPON 828

Figure 3 Chemical structure of Epon 828; 85% $n = 0$ and 15% $n = 1$ species.

and a tensile force was applied. Universal joints above and below the sample holders were used to aid in alignment. A crosshead speed of 0.05 cm min^{-1} was used. Fig. 5 illustrates the tension/shear test geometry and Fig. 6 is a photograph of the experimental apparatus. Equations 1 and 2 describe the angular dependence of the shear stress, τ, and tensile normal stress, σ, respectively:

$$\tau = \frac{P}{A}\cos\theta \quad (1)$$

$$\sigma = \frac{P}{A}\sin\theta \quad (2)$$

where P is the applied load and A is the interfacial area. Note that A is constant for all of the samples.

Compressive normal/shear stress testing was accomplished by immobilizing the epoxy and PBT/epoxy samples in two identically milled steel blocks. These steel blocks were placed in a cage designed in such a way that a tensile force could be applied and measured by a load cell while a compressive deformation was applied to the sample. Once again a crosshead speed of 0.05 cm min^{-1} was employed. Note that in addition to a universal joint, a $\frac{1}{2}$ in. steel ball was placed into a hemispherical depression which was milled on the bottom of one of the steel blocks. This was done to further aid in alignment. The compression/shear test geometry and experimental apparatus are shown in Figs 7 and 8, respectively. Equations 1 and 2 also apply for compressive normal/shear stress testing except that σ becomes negative. Angles of 35 and 45° were investigated for compression/shear testing.

The fracture surface of each sample was examined using optical microscopy. A typical sample was chosen for viewing in an ETEC Autoscan scanning electron microscope (SEM). Samples were coated with 35 nm of gold/palladium prior to observation in order to minimize charging. The SEM was operated at an accelerating voltage of 10 kV.

4. Results

The fracture loads were measured for both the epoxy and PBT/epoxy samples at each angle for each cure temperature. Six PBT/epoxy and four epoxy samples were tested at each condition. Using Equations 1 and 2 the fracture loads where converted into stresses τ and σ, respectively. Figs 9 to 12 show plots of τ against σ for the samples cured at 55, 85, 115 and 215° C, respectively.

Absent from Figs 9 to 12 are the data on the neat epoxy samples tested in compression/shear. These samples did not fracture when loaded to 450 kg, the capacity of the load cell. This loading corresponded to a maximum shear and compressive normal stress of 37 and 26 MPa, respectively, for the 35° samples. Similarly, for the 45° samples the maximum shear and compressive normal stress experienced was 32 MPa.

Such combined stress testing data are amenable to analysis using failure criteria. Many lamina strength failure criteria have been derived for composite materials. Among these are a maximum stress, maximum strain and quadratic interaction criteria [20]. The maximum stress and strain failure criterion predict failure when any stress or strain component reaches its ultimate value. The quadratic interaction type criterion takes into account the interaction of stresses in a biaxial stress field.

Tsai and Wu have proposed a general strength criterion for the failure of anisotropic materials subjected to multi-axial stresses [21]. It assumes that the stress-space failure surface can be described by a scalar function of two strength tensors. By using a criterion based upon strength tensors it is possible to satisfy the transformation relations of tensors. For plane states of stress this criterion can be simplified to the following:

$$F_1\sigma_1 + F_2\sigma_2 + F_6\sigma_6 + F_{11}\sigma_1^2 + 2F_{12}\sigma_1\sigma_2 + F_{22}\sigma_2^2 + F_{66}\sigma_6^2 = 1 \quad (3)$$

where σ_1 is the normal stress in the (1) direction, σ_2 the normal stress in the (2) direction, and σ_6 the shear

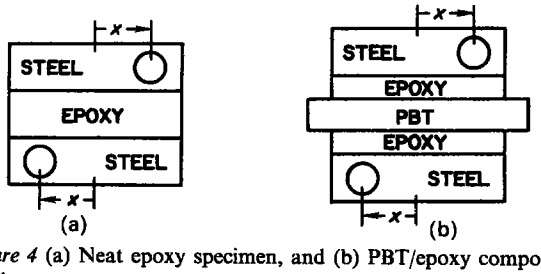

Figure 4 (a) Neat epoxy specimen, and (b) PBT/epoxy composite specimen.

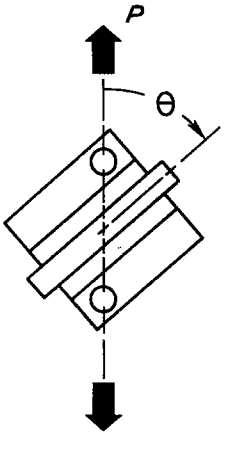

Figure 5 Schematic drawing of tensile normal/shear stress geometry.

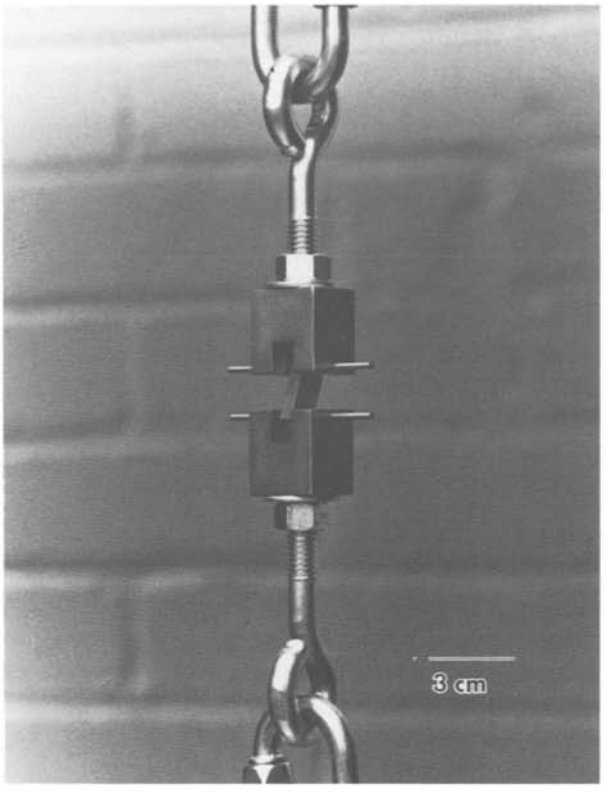

Figure 6 Photograph of tension/shear experimental apparatus.

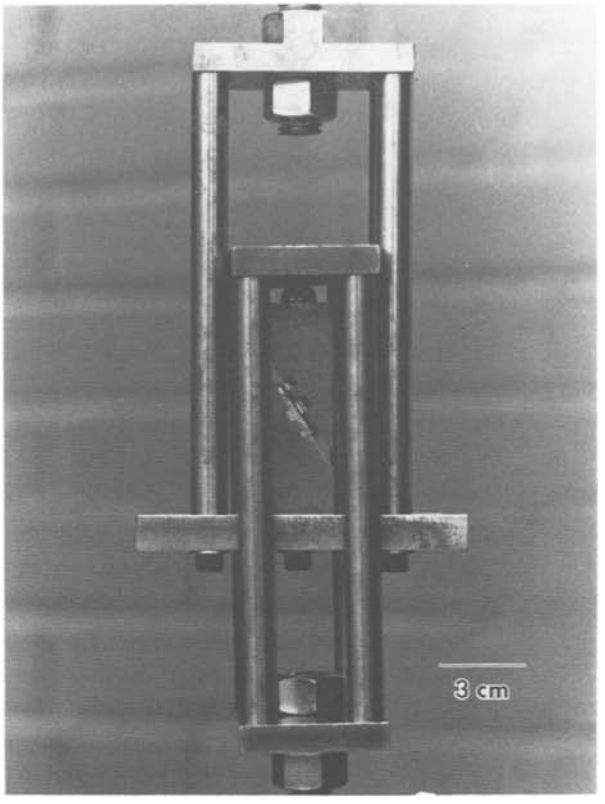

Figure 8 Photograph of the compression/shear experimental apparatus.

stress in the (1–2) direction. All of the coefficients in Equation 3 can be expressed in terms of the ultimate adhesive strengths of the material:

$$F_1 = 1/\sigma_1^T - 1/\sigma_1^C$$
$$F_2 = 1/\sigma_2^T - 1/\sigma_2^C$$
$$F_6 = 1/\tau^+ - 1/\tau^-$$
$$F_{11} = 1/\sigma_1^T\sigma_1^C$$
$$F_{22} = 1/\sigma_2^T\sigma_2^C$$
$$F_{66} = 1/(\tau^+\tau^-)$$

where σ_1^T is the ultimate tensile adhesive strength in the (1) direction, σ_1^C the ultimate compressive adhesive strength in the (1) direction, σ_2^T the ultimate tensile adhesive strength in the (2) direction, σ_2^C the ultimate compressive adhesive strength in the (2) direction, τ^+ the ultimate positive in-plane (1–2) adhesive shear strength, τ^- the ultimate negative in-plane (1–2) adhesive shear strength.

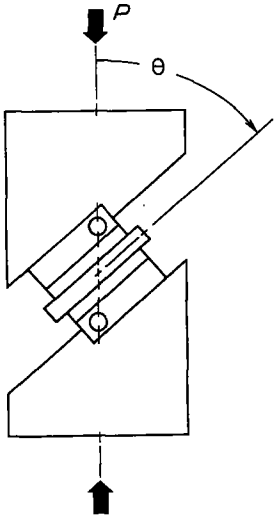

Figure 7 Schematic drawing of normal compressive/shear stress geometry.

Based on stability considerations Tsai and Wu [21] have suggested that $F_{12} = 0$. Since $\sigma_2 = 0$ for these experiments, Equation 3 can be simplified to Equation 4:

$$F_1\sigma_1 + F_6\sigma_6 + F_{11}\sigma_1^2 + F_{66}\sigma_6^2 = 1 \quad (4)$$

Assuming the positive and negative in-plane adhesive shear strengths to be the same yields Equations 5 and 6:

$$F_6 = 0 \quad (5)$$

$$F_1\sigma_1 + F_{11}\sigma_1^2 + F_{66}\sigma_6^2 = 1 \quad (6)$$

If the ultimate compressive adhesive strength is taken as ∞ then the following simplifications can be made:

$$F_1 = 1/\sigma_1^T = 1/\sigma_0$$
$$F_{11} = 0$$

This leads to the failure criterion given in Equation 7:

$$F_1\sigma_1 + F_{66}\sigma_6^2 = 1 \quad (7)$$

Letting $\sigma_1 = \sigma$, $\sigma_6 = \tau$ and $\tau^+ = \tau_0$, Equation 7 may be equivalently written as:

$$\sigma/\sigma_0 + \tau^2/\tau_0^2 = 1 \quad (8)$$

Rearranging Equation 8 yields:

$$\tau^2 = \tau_0^2 - (\tau_0^2/\sigma_0)\sigma \quad (9)$$

From such an analysis two intrinsic adhesive strengths can be predicted. These are σ_0, the adhesive strength

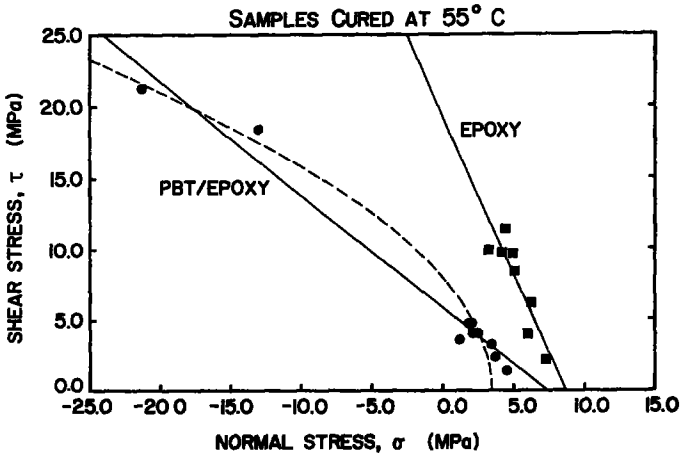

Figure 9 Plot of τ against σ for the epoxy and PBT/epoxy samples cured at 55° C. The dashed line is the least-squares fit of the data using a modified Tsai–Wu failure criterion. The solid line is the least-squares fit using a Coulomb-type failure criterion.

in the absence of shear stress and τ_0, the adhesive strength in the absence of normal stress. In addition to σ_0 and τ_0, Equation 9 can be used to determine the sensitivity of the adhesive strength to the degree of normal stress. While information of this kind is important in the design of composite structures, such adhesive data are difficult to find in the literature. Performing a least-squares fit of the PBT/epoxy data using the modified Tsai–Wu failure criterion given in Equation 9 results in the dashed lines plotted on Figs 9 to 12. The agreement between the data and the fit is good.

For comparison, a least-squares fit of the epoxy and PBT/epoxy data is also plotted using a Coulomb-type failure criterion [22]. Derived for the fracture of soils, it assumes a shear failure. This criterion has been suggested by Kadotani and Aki [23] for the fracture of mica/epoxy composites. The Coulomb-type failure criterion is given by Equation 10:

$$\tau = \tau_0 - \mu\sigma \tag{10}$$

where τ_0 is the intrinsic adhesive shear strength and μ is a frictional coefficient which describes the dependence of the adhesive strength on the degree of normal stress σ. The intrinsic adhesive strength in the absence of shear stress may be determined by evaluating the ratio of τ_0/μ.

Table II summarizes the results of the least-squares analyses using the modified Tsai–Wu and the Coulomb-type failure criteria. The Tsai–Wu criterion fits the PBT/epoxy data better. Using this failure criterion adhesive strengths of 3.5 and 8.2 MPa were predicted in the absence of shear and normal stress, respectively for the PBT/epoxy samples cured at 55° C. It appears that the Coulomb-type criterion overestimates both the ultimate tensile adhesive strength and the effect of compressive normal stress for the composite samples.

5. Discussion

Optical microscopy and SEM were used to study the resulting fracture surfaces after testing. From these observations it was possible to qualitatively ascertain whether the fractures were the result of cohesive or adhesive failures. The neat epoxy fractures were both adhesive and cohesive; i.e. there was a debonding from the steel substrate as well as a cohesive fracture of the epoxy. Figs 13a and b are SEI of a typical epoxy fracture surface.

In contrast to the neat epoxy fractures, the composite fractures were primarily adhesive; i.e. there was a relatively clean delamination of the PBT ribbon from the epoxy. An SEI of a cleanly delaminated PBT ribbon and a corresponding epoxy fracture surface are shown in Figs 14a and b. Note how the epoxy forms a negative replica of the PBT surface. For comparison, an SEI of the as-extruded PBT ribbon is shown in Fig. 14c. The oval surface depressions, which are oriented in the extrusion direction, are believed to be induced during the extrusion processes. In limited

TABLE II A summary of the adhesive parameters determined by a least-squares fit of the epoxy and PBT/epoxy data using a modified Tsai–Wu and a Coulomb-type failure criterion

Sample	Modified Tsai–Wu criterion			Coulomb-type criterion			
	τ_0 (MPa)	σ_0 (MPa)	Correl. coeff.	τ_0 (MPa)	σ_0 (MPa)	μ	Correl. coeff.
55° C cure							
Epoxy	–	–	–	19.4	8.6	2.25	−0.884
PBT/epoxy	8.2	3.5	−0.993	5.8	7.3	0.80	−0.987
85° C cure							
Epoxy	–	–	–	14.9	11.8	1.26	−0.951
PBT/epoxy	6.4	3.1	−0.993	4.9	6.8	0.72	−0.980
115° C cure							
Epoxy	–	–	–	20.9	10.6	1.96	−0.892
PBT/epoxy	6.4	3.4	−0.997	5.0	6.9	0.72	−0.976
215° C cure							
Epoxy	–	–	–	27.2	8.3	3.25	−0.973
PBT/epoxy	6.0	3.0	−0.993	4.7	6.5	0.72	−0.992

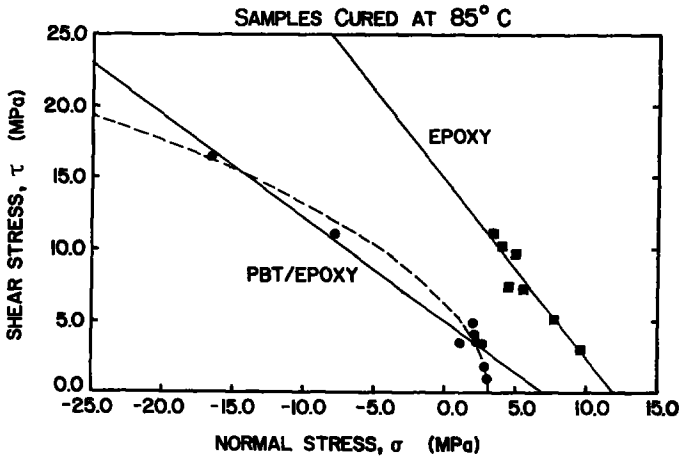

Figure 10 Plot of τ against σ for the epoxy and PBT/epoxy samples cured at 85° C. The dashed line is the least-squares fit of the data using a modified Tsai–Wu failure criterion. The solid line is the least-squares fit using a Coulomb-type failure criterion.

areas, there was cohesive fracture of the PBT ribbon as indicated by fibrillation, together with adhesively fractured surfaces. Figs 15a and b are SEI of such mixed-mode fracture morphologies. The composite fracture surfaces showed no evidence of any epoxy fracture or debonding from the steel substrate. This observation is in agreement with the results presented in Figs 9 to 12.

Figs 9 to 12 indicate that the degree of adhesion between PBT and epoxy is low. This may, however, be advantageous in filament-wound composites where release agents are sometimes used to minimize fibre–matrix adhesion. For applications which require high adhesive strengths it might be possible to superimpose a compressive normal stress across the PBT/epoxy composite interface via design or manufacturing modifications. Such approaches would effectively increase the apparent adhesive strength.

From Table II the adhesive strengths determined by a least-squares analysis using the modified Tsai–Wu failure criterion suggest that adhesive strength decreases with increasing cure temperature. It would be expected that the degree of chemical adhesion should increase with cure temperature or at least remain the same. If this is true for the PBT/epoxy system, then some other effect must be present which predominates over the effect of chemical adhesion in order to explain the observed decrease in adhesive strength with cure temperature. Assuming no change in chemical adhesion with cure temperature then residual stresses may explain the observed adhesive behaviour. Ongoing epoxy cure research on the neat V-40/828 system by Vratsanos and Farris [18, 19] suggests that the residual cure and thermal stress at room temperature is least for the 55° C cure. Greater residual stresses are generated at the higher cure temperatures. The 85 and 115° C cure temperatures result in almost identical room temperature residual stress behaviour. 215° C cures would be expected to have the greatest residual stresses at room temperature. Epoxy degradation, which also takes place at this cure temperature, increases the residual stress. For all cure temperatures it has been shown that cure stresses were negligibly small in comparison to thermal stresses [18, 19].

Upon cooling from the cure temperature in-plane thermal stresses are generated in each layer of the samples. By virtue of the sample geometry there are no thermal stresses which act through the thickness, i.e. across the steel/epoxy or PBT/epoxy interface. From a linear thermoelastic model it is easy to show that since the steel substrate is present in such a large amount it is free to expand and contract with temperature. Fig. 16 schematically illustrates the thermal stress behaviour for the composite samples as a result of the constraint imposed by the steel substrate. Assuming the steel to be stress-free, Equations 11 and 12 approximately express the thermal strains in the epoxy ε_{Ep} and PBT ε_{PBT} layers, respectively:

$$\varepsilon_{Ep} = (\alpha_{Ep} - \alpha_{St})(T_{Cure} - T_{Room}) \quad (11)$$

$$\varepsilon_{PBT} = (\alpha_{PBT} - \alpha_{St})(T_{Cure} - T_{Room}) \quad (12)$$

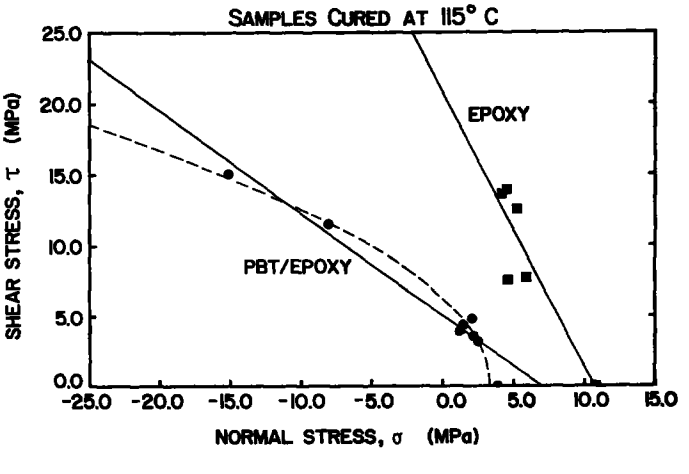

Figure 11 Plot of τ against σ for the epoxy and PBT/epoxy samples cured at 115° C. The dashed line is the least-squares fit of the data using a modified Tsai–Wu failure criterion. The solid line is the least-squares fit using a Coulomb-type failure criterion.

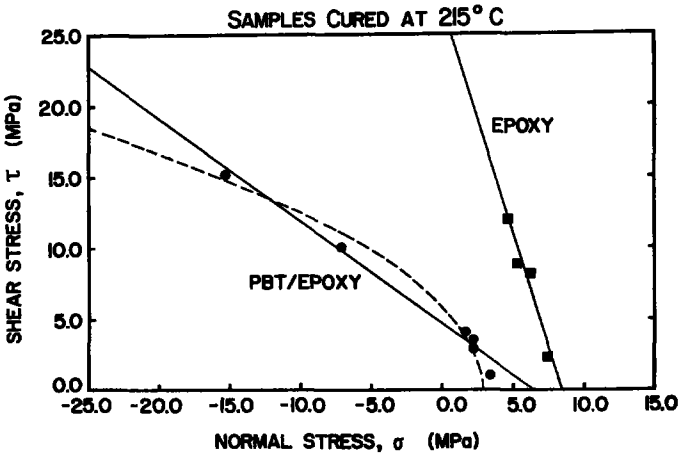

Figure 12 Plot of τ against σ for the epoxy and PBT/epoxy samples cured at 215° C. The dashed line is the least-squares fit of the data using a modified Tsai–Wu failure criterion. The solid line is the least-squares fit using a Coulomb-type failure criterion.

where

$\alpha_{Ep} = 5 \times 10^{-5}\,°C^{-1}$ = linear thermal expansion coefficient of epoxy

$\alpha_{PBT} = -1 \times 10^{-6}\,°C^{-1}$ = linear thermal expansion coefficient of PBT [24]

$\alpha_{St} = 1 \times 10^{-5}\,°C^{-1}$ = linear thermal expansion coefficient of steel

T_{Cure} = 55, 85, 115 or 215° C

T_{Room} = 20° C

Table III summarizes the thermal strains predicted in these experiments using this simple thermoelastic model. Multiplying the tensile modulus of PBT with the thermal strains in Table III gives an approximate measure of the thermal stress in the PBT film as a function of cure temperature. From Table I, the compressive stress needed to buckle PBT is 230 MPa. Thus a ΔT of 195° C (cure temperature of 215° C) is large enough to thermally induce compressive buckling. Cure temperatures over 200° C can easily be realized commercially since many of the thermosetting matrices now employed in high performance applications require post-curing at elevated temperatures. Since Kevlar fibres have compressive buckling characteristics similar to that of PBT, thermally induced buckling may also be expected for Kevlar composites. Similarly, PBT or Kevlar composites using high-melting thermoplastics such as poly(ether ether ketone) (PEEK) as a matrix may suffer from the same buckling problems.

Work by DeTeresa [14] on the compressive behaviour of high-performance fibres has shown that PBT fibres form distinct periodic kink bands which bulge from the surface. A similar, but not quite as distinct, non-periodic bulging occurs with the compression of PBT films. Fig. 17 is an SEI of a fractured PBT/epoxy

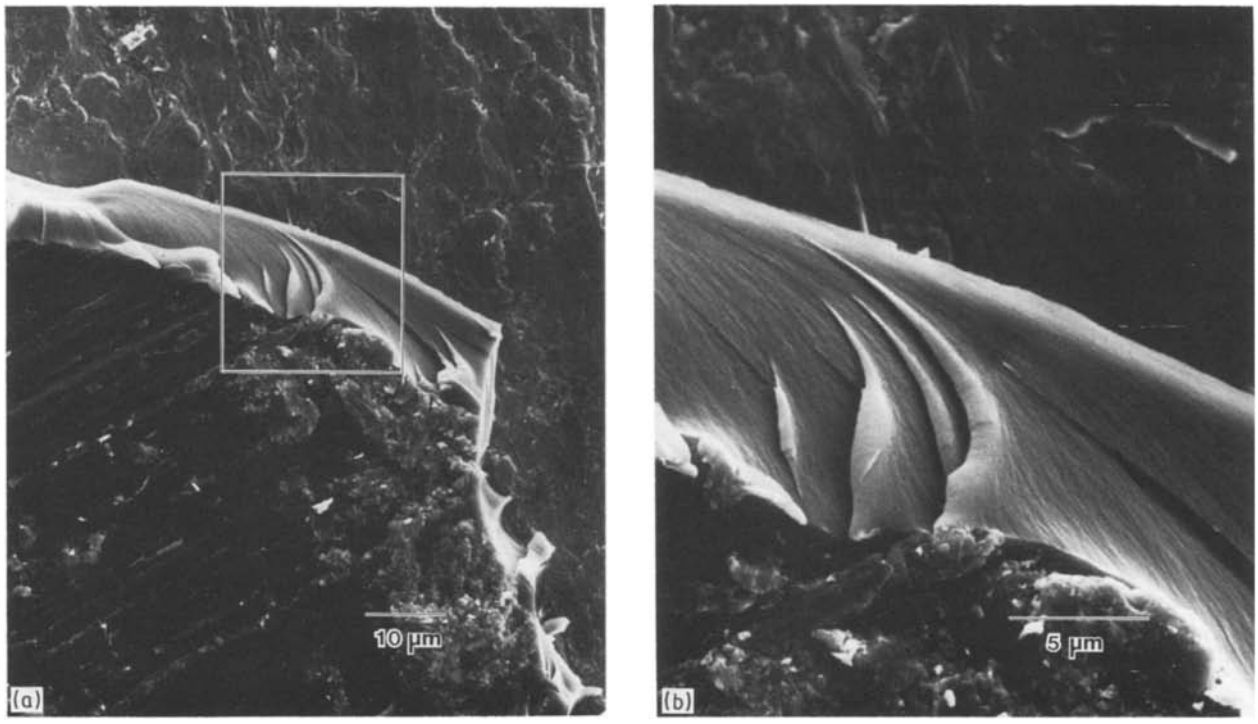

Figure 13 Secondary electron image (SEI) of a typical neat epoxy fracture surface at (a) low magnification showing both debonding from the steel substrate and cohesive fracture of the epoxy, and (b) an enlargement of the region outlined in (a).

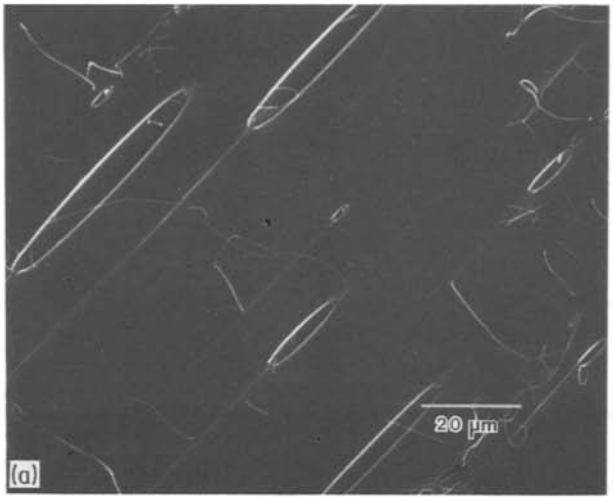

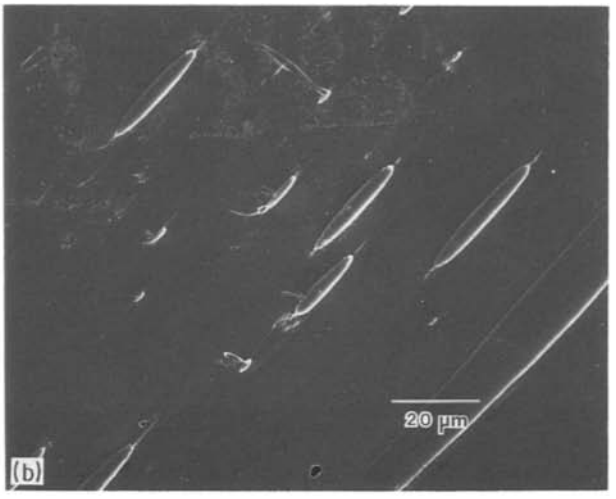

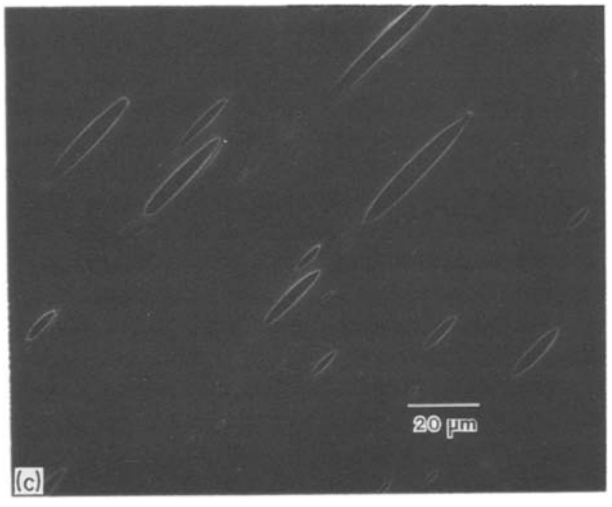

Figure 14 SEI of (a) a PBT/epoxy adhesive fracture showing a cleanly delaminated PBT ribbon, (b) a corresponding epoxy fracture surface showing that it forms a negative replica of the PBT surface, and (c) the as-extruded PBT ribbon. The oval surface depressions, which are oriented along the extrusion direction, are the result of the extrusion process.

sample showing these thermally induced compressive kink bands on the surface of the PBT ribbon. Since the onset of buckling occurs when the epoxy is glassy, it is no longer possible for the epoxy to conform to the PBT surface. Thus, in order for the kink bands to form it may be necessary for the PBT film to locally delaminate from the epoxy. The stresses required to fracture the PBT/epoxy interface under these conditions would be less as compared to fracturing a non-buckled PBT/epoxy interface. While this may help explain the decrease in adhesive strength for the PBT/epoxy samples cured at the 215° C cure temperature, it is difficult, however, to differentiate among the effects of buckling, residual stress or epoxy degradation on the adhesive behaviour. One possible way these effects could be isolated would be to use substrates of higher thermal expansion coefficient than steel. Compressive buckling could then be induced at lower temperatures where the thermal stress behaviour would be known and the epoxy would not degrade. Similarly, one could vary the curing time at 215° C. Since the thermal stress is independent of cure time, it would be possible to vary the residual stress due to degradation. Further work in this area is required.

TABLE III Resulting room temperature thermal strains in the epoxy ε_{Ep} and PBT ε_{PBT} layers for each cure temperature as a result of cooling from the cure temperature

Cure temperature (° C)	ε_{Ep} (10^{-3})	ε_{PBT} (10^{-3})
55	1.4	−0.4
85	2.6	−0.7
115	3.8	−1.1
215	7.8	−2.2

The relatively low adhesive strengths for PBT/epoxy composites suggest that secondary bonds such as van der Waals interactions or mechanical adhesion may be responsible for the observed degree of adhesion between PBT film and epoxy. Mammone and Uy [12] have suggested that secondary bonds are responsible for the adhesion of PBT fibres to epoxy. This is not surprising when one considers that PBT is nearly chemically and thermally inert under the conditions used in these experiments. In an attempt to increase the surface polarity of PBT, Mammone and Uy etched PBT fibre in a sulphuric acid solution. However, the resulting acid-etched PBT/epoxy composites showed no improvement in interlaminar shear strength over untreated PBT/epoxy composites [12]. With regard to adhesion, if PBT is similar to other high-performance reinforcements then improvements in adhesive strength might only result from severe surface treatments such as corona or plasma etches [25, 26].

An alternative explanation to the low adhesive strengths measured is the fact that these composites offer a simple fracture path. If there is any local delamination it would be expected that the propagation of the delamination would be rapid. This is in contrast to the path available to delamination in composite structures based upon PBT fibres where delamination might be arrested locally by virtue of the composite microstructure. Such explanations, however, do not account for the discrepancy between the adhesive strengths reported here and by others [12, 13] for PBT/epoxy composites. It should be noted, however, that the adhesive strengths measured by the short

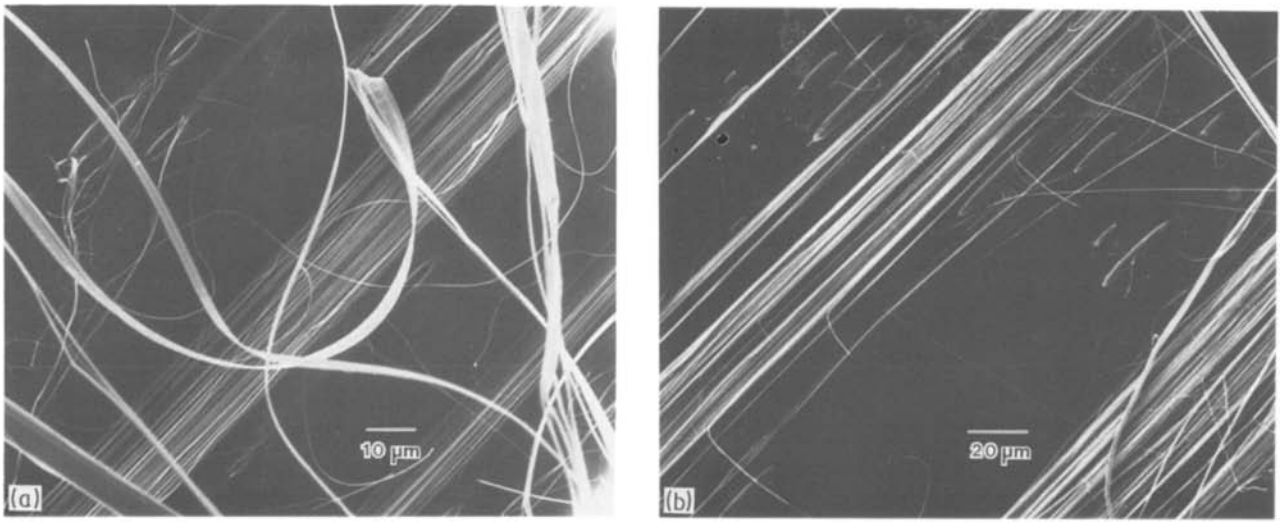

Figure 15 SEI of mixed-mode fracture morphologies of PBT/epoxy composites showing (a) a delaminated PBT ribbon with some regions of cohesively fractured PBT as evidenced by fibrillation, and (b) a corresponding adhesively fractured epoxy surface with some surface fibrils of PBT attached.

beam shear test used in the other PBT/epoxy studies have not been corrected for the effect of compressive normal stress or load transfer. As shown in Figs 9 to 12 the effect of compressive loading can be significant.

Comparing the modified Tsai–Wu fit of the data with the Coulomb-type fit indicates that the frictional coefficient μ, derived from the Coulomb analysis, is an average dependence of the adhesive strength on the normal stress. For PBT/epoxy composites the use of the Coulomb criterion can lead to errors at large tensile and compressive normal stresses. Thus, it is not surprising then that μ of the PBT/epoxy composites appears to be insensitive to cure temperature. By comparison, the neat epoxy samples are more sensitive to normal stress at all four cure temperatures. The effect of compressive normal stress on the adhesive performance of a composite is similar to the effect of interfacial pressure which can develop between fibre and matrix during the cure process [27]. A similar analogy may be drawn for tensile normal stress and any interfacial tension which may develop due to cure.

6. Conclusions

A simple test method, based upon a modified scarf joint specimen, was developed in order to measure adhesive strengths in the presence of normal (tensile or compressive) and shear stresses. In addition, this method permits determinations of the sensitivity of the adhesive strength to the degree of normal stress. The experimental method included the use of both tensile and compressive normal stresses in combination with shear stresses. This test method was applied to epoxy and PBT/epoxy composites.

A modified Tsai–Wu failure criterion accurately describes the adhesive failure envelope of PBT/epoxy composites. This criterion predicts adhesive strengths of 3.5 and 8.2 MPa in the absence of shear and normal stress, respectively, for these composites. Tensile normal stresses were found to be deleterious to the performance of these composites. A decrease in adhesive strength with cure temperature was attributed to residual cure and thermal stresses.

The mechanism of adhesion between PBT and epoxy is via secondary bonds and mechanical adhesion. As a result, the fracture of these composites is predominantly adhesive with delamination of the PBT from the epoxy.

Future work will investigate the effects of surface treatment, residual stress and hydrostatic pressure on the adhesive behaviour of PBT/epoxy composites.

Acknowledgement

The authors wish to acknowledge the financial support of the United States Air Force under contract AF-F33615-82-K-5068.

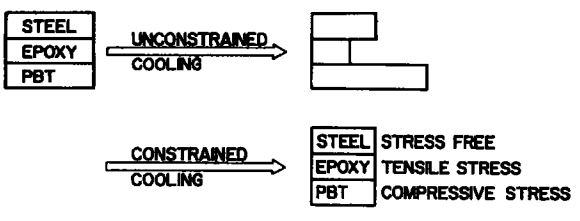

Figure 16 Schematic drawing of the thermal stress behaviour for the PBT/epoxy composite for unconstrained and constrained cooling.

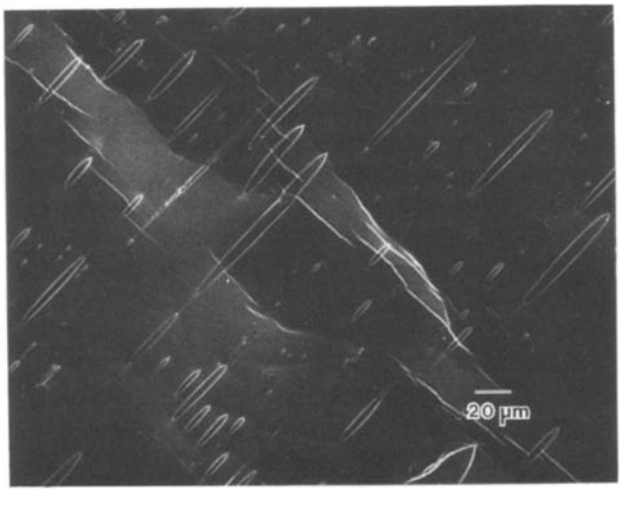

Figure 17 SEI of fractured PBT/epoxy composite cured at 215° C showing PBT film with thermally induced compressive kink bands.

References

1. L. YING, *SAMPE Q.* **14** (1983) 26.
2. L. T. DRZAL, J. A. MESCHER and D. L. HALL, *Carbon* **17** (1979) 375.
3. L. T. DRZAL, M. J. RICH, J. D. CAMPING and W. J. PARK, Technical Report AFWAL-TR-81-4003, "Interfacial Shear Strength and Failure Mechanisms in Graphite Fiber Composites" (1981).
4. L. S. PENN, F. A. BYSTRY and H. J. MARCHIONNI, *Polym. Compos.* **4** (1983) 26.
5. P. E. SANDORFF, *J. Compos. Mater.* **14** (1980) 199.
6. M. ARCAN, Z. HASHIN and A. VOLOSHIN, *Exp. Mech.* **18** (4) (1978) 141.
7. S. R. ALLEN, R. J. FARRIS and E. L. THOMAS, *J. Mater. Sci.* **20** (1985) 2727.
8. *Idem, ibid.* **20** (1985) 3643.
9. L. FELDMAN, R. J. FARRIS and E. L. THOMAS, *ibid.* **20** (1985) 2719.
10. E. C. CHENEVEY, Technical Report AFWAL-TR-80-4142, "Processing of Rod Like Polymers", Part III (1982).
11. *Idem*, Technical Report AFWAL-TR-80-4142, "Processing of Rod Like Polymers", Part IV (1984).
12. J. F. MAMMONE and W. C. UY, Technical Report AFWAL-TR-82-4154, "Exploratory Development of High Strength, High Modulus Polybenzothiazole Fibers: Fiberization Scale-Up and Optimization", Part II (1984).
13. E. C. CHENEVEY, Technical Report AFWAL-TR-82-4194, "High-Strength High-Modulus Polybenzothiazole (PBT) Fiber", Part II (1985).
14. S. J. DETERESA, PhD thesis, University of Massachusetts (1985).
15. C. A. MAY and Y. TANAKA (eds), "Epoxy Resins Chemistry and Technology" (Marcel Dekker, New York, 1973).
16. D. E. FLOYD, "Polyamide Resins", 2nd Edn (Reinhold, New York, 1966).
17. J. K. RASMUSSEN and H. K. SMITH II, *J. Appl. Polym. Sci.* **28** (1983) 2473.
18. M. S. VRATSANOS and R. J. FARRIS, *J. Appl. Polym. Sci.* (in press).
19. M. S. VRATSANOS and R. J. FARRIS, in "Composite Interfaces", Vol. 1, edited by H. Ishida and J. L. Koenig (Elsevier, New York, 1986) p. 71.
20. J. M. WHITNEY, I. M. DANIEL and R. B. PIPES, Experimental Mechanics of Fiber Reinforced Composite Materials, Society for Experimental Stress Analysis (1982).
21. S. W. TSAI and E. M. WU, *J. Compos. Mater.* **5** (1971) 58.
22. J. C. JAEGER and N. G. W. COOK, "Fundamentals of Rock Mechanics" (Methuen, London, 1969).
23. K. KADOTANI and F. AKI, *Composites* **15** (1984) 57.
24. L. A. POTTICK, S. R. ALLEN and R. J. FARRIS, *J. Appl. Polym. Sci.* **29** (1984) 3915.
25. R. E. ALLRED, E. W. MERRILL and D. K. ROYLANCE, ACS, Division of Polymer Chemistry, Polymer Preprints 24 (1) (1983) p. 223.
26. N. H. SUNG, G. DAGLI and L. YING, Proceedings of the 37th Annual Technical Conference, RP/C, SPI, Washington, DC, Section 23-B (1982) p. 18.
27. B. HARRIS, *J. Mater. Sci.* **13** (1978) 173.

Received 4 March
and accepted 22 May 1986